

Spin susceptibility and pseudogap in $\text{YBa}_2\text{Cu}_4\text{O}_8$: An approach via a charge-density-wave instability

I. Eremin, M. Eremin, and S. Varlamov

Physics Department, Kazan State University, 420008 Kazan, Russia

D. Brinkmann, M. Mali, and J. Roos

Physik-Institut, University of Zürich, CH-8057 Zürich, Switzerland

(Received 27 January 1997; revised manuscript received 12 June 1997)

The temperature dependence of the spin susceptibility in $\text{YBa}_2\text{Cu}_4\text{O}_8$ has been calculated on the assumption that a pseudogap in the normal state opens due to a charge-density-wave (CDW) instability. The agreement with experiment is very good. The doping dependence of the pseudogap forming temperature is discussed. The model also predicts an isotope effect of the CDW forming temperature and peculiar features of the Fermi surface. [S0163-1829(97)07241-X]

I. INTRODUCTION

The peculiar temperature dependence of the spin susceptibility of high- T_c superconductors is far from being completely understood (see, for example, Ref. 1 and references therein). For instance, the strong temperature dependence of the susceptibility in $\text{YBa}_2\text{Cu}_4\text{O}_8$ is believed to arise from the opening of a so-called “spin gap” in the excitation spectrum at a temperature $T_S \approx 150$ K which is above the superconducting transition temperature, T_c . Recently, evidence for the opening of a pseudogap in the normal state of underdoped $\text{Bi}_2\text{Sr}_2\text{CaCu}_2\text{O}_{8+y}$ was found by photoemission spectroscopy.^{2,3} The nature of the spin gap and pseudogap are not clear yet and it is under intensive debate in the literature. In particular, by comparing the temperature dependences of the spin susceptibility and the specific heat in $\text{YBa}_2\text{Cu}_3\text{O}_{7-y}$ it has been concluded⁴ that the spin and charge excitations do not separate in the normal state in YBCO compounds which, in this context, behave like ordinary Fermi liquids.

A clue to the origin of the pseudogap phenomenon may be found in the following fact. In $\text{YBa}_2\text{Cu}_4\text{O}_8$, which is regarded to be the most stable and homogeneous compound in the YBCO family, several structure related anomalies have been observed around a temperature $T^* \approx 180$ K, namely by Raman scattering,⁵ x-ray diffraction,⁶ and nuclear magnetic resonance (NMR) and/or nuclear quadrupole resonance (NQR).⁷⁻⁹ These anomalies seem to support the idea¹⁰ that the spin gap phenomenon is caused, at least partly, by a transition due to a charge density wave (CDW).

It is known that a quasi-two-dimensional (2D) metal with strong anisotropic Fermi surface is unstable with respect to a CDW transition.^{11,12} According to photoemission data (see the review in Ref. 13), Fermi surfaces in layered cuprates are really different from a perfect circle or cylinder. Therefore, the analysis of the CDW scenario as a possible origin for the opening of a pseudogap in the normal state is desirable. This point has been emphasized by many authors (for example, Refs. 14–16), however, to our knowledge, numerical calculations have not been performed.

In this paper, we pursue the CDW approach and present the exact numerical solution of the integral equations for the CDW gap and its dependence on temperature and momentum. We then calculate the temperature dependence of the susceptibility for the range $T_c < T < T^*$ and compare the result with experimental Cu(2) Knight shift data¹⁷ for $\text{YBa}_2\text{Cu}_4\text{O}_8$. Finally, we consider the doping and the isotope dependence of T^* .

II. MODEL HAMILTONIAN

We start from the usual t - J model Hamiltonian:

$$H = \sum_k t_k \Psi_k^{pd,\sigma} \Psi_k^{\sigma,pd} + \sum_{ij} J_{ij} \left[(\vec{S}_i \vec{S}_j) - \frac{n_i n_j}{4} \right] - \sum_i F_i (S_{i+1} + S_{i+2} + S_{i+3} + S_{i+4})^2, \quad (1)$$

where $\Psi_k^{pd,\sigma}$, $\Psi_k^{\sigma,pd}$ are quasiparticle Hubbard-like operators for the copper-oxygen singlet band,^{18,19} J_{ij} is the superexchange constant of the copper spin coupling, n_i is the number of copper spins, and F_i is the relatively small parameter of the spin polarization around the Zhang-Rice singlet at site i (Ref. 20).

For simplicity, we omit the coupling between singlet and copper bands²¹ and describe the energy dispersion by

$$\varepsilon_k = P t_k - \mu, \quad (2)$$

where P is the thermodynamic average of the anticommutator $[\Psi_k^{pd,\sigma}, \Psi_k^{\sigma,pd}]_+$, t_k are hopping integrals:

$$t_k = 2t_1 [\cos(k_x) + \cos(k_y)] + 4t_2 \cos(k_x) \cos(k_y) + 2t_3 [\cos(2k_x) + \cos(2k_y)] \quad (3)$$

with t_1 , t_2 , and t_3 referring to hopping to the first, second, and third Cu neighbors, respectively.

The largest parameter, t_1 , can be estimated as 70 meV from the bandwidth which was measured by photoemission spectroscopy.²² The position of the saddle singularity peak in the density of states (DOS) with respect to the Fermi level is

TABLE I. Q vector of the maximum of $\chi_L(Q)$ and correlation length ξ_0 at $T=150$ K (in units of the lattice constant a).

δ	0.10	0.33	0.5
ξ_0	1.6	1.3	1.4
(Q_x, Q_y)	$(0, \pm \pi); (\pm \pi, 0)$	$(\pm \pi, \pm \pi)$	$(\pm \pi, \pm 2\pi/3); (\pm 2\pi/3, \pm \pi)$

given by $4P(t_3 - t_2)$ and should be 19 meV.²² If, in addition, we take into account the pseudogap in the normal state, which is 20 meV,^{2,3} we can expect $t_3 - t_2$ to be 3–5 meV at most. For simplicity, we assume $t_2 = 0$ and $t_3 = 5$ meV.

The chemical potential μ was calculated self-consistently from the equation

$$\delta = \frac{P}{N} \sum f(\epsilon_k), \quad (4)$$

where δ is a doping parameter which denotes the number of doped holes per unit cell in bilayer Cu_2O_4 and $f(\epsilon_k)$ is the usual Fermi function.

These parameters describe quite well the experimentally observed anisotropy of the Fermi surface in an untwinned crystal of $\text{YBa}_2\text{Cu}_3\text{O}_{6.95}$ if we choose $\delta \approx 0.33$, which is a reasonable value.

Using one band t - J model, we suppose that the bonding and antibonding plane bands are separated due to interplane coupling and the antibonding band is almost empty. The energy splitting between the saddle singularity peaks around 300 meV in $\text{YBa}_2\text{Cu}_4\text{O}_8$ follows from recent band calculations.²³ Experimental evidence for the splitting in untwinned crystals of $\text{YBa}_2\text{Cu}_3\text{O}_{6.95}$ has been obtained recently.²⁴ Although the question about the value of interplane splitting is not yet resolved, the present results on the Fermi surface anisotropy provide a sound basis for the investigation of various aspects of the CDW or SDW (spin density wave) instability.

We want to determine the instability vector, Q , on the basis of the preliminary calculations of the Lindhard response function:

$$\chi_L(Q) = \frac{P}{N} \sum \frac{f(\epsilon_k) - f(\epsilon_{k+Q})}{\epsilon_k - \epsilon_{k+Q}}. \quad (5)$$

In Table I, we present the values $\chi_L(Q)$ for three doping levels. As expected,¹⁰ close to half-filling ($\delta = 0.33$) the response function reaches a maximum around $Q = (\pi, \pi)$. If δ decreases, the maximum $\chi_L(Q)$ shifts along the boundary of the Brillouine zone and for $\delta = 0.1$, corresponds to the points $Q = (\pm \pi, 0)$ and $(0, \pm \pi)$.

For $\delta = 0.33$, Eq. (4) yields $\mu = 0$. The calculated DOS is presented in Fig. 1 where we employ the ‘‘hole picture’’ (in contrast to Ref. 22).

The correlation length, ξ_0 , was calculated using the relation

$$\langle \Psi_i^{pd, \sigma} \Psi_j^{\sigma, pd} \rangle \propto \exp\left(-\frac{|R_{ij}|}{\xi_0} + iQR_{ij}\right), \quad (6)$$

the results are given in Table I. Since the correlation length is not too large, the mean-field approximation can be quite applicable for our analysis. For the temperature range 50–

300 K, ξ_0 is almost independent from temperature, which contrasts with the quasi-1D case where $\xi_0^{1d} \propto 1/T$.¹²

We note here that, for decreasing δ , the correlation length, ξ_0 , has a tendency to be quasidegenerate. For δ about 0.1, two quasi-1D CDW’s are possible, one along the a the other along the b axis. That situation, which we will not treat here, is complicated by phase fluctuations which, as a rule, are very important in 1D systems.²⁵

In the present paper, using a mean-field approximation, we will study the nature of the two-dimensional instability of the Cu_2O_4 bilayer for the half-filling regime, that is for $0.25 < \delta < 0.45$. It has been pointed out by many authors (for example, Refs. 26 and 27, and references therein), that the mean-field approximation may be applicable for even quasi-1D systems if the coupling between chains is strong enough, although the mean-field parameters will be affected by fluctuations. In this context, we may expect that calculated mean-field transition temperature, T^* , will be slightly washed out by phase fluctuations of the order parameter.

III. CDW PSEUDOGAP FUNCTION

We now take into account the quasiparticle interactions mediated by the phonon field; this leads to the CDW transition. The interaction can be written as follows:

$$H_{\text{CDW}} = \sum [G_0(Q) + G_1(k, Q)] \Psi_{k-Q}^{pd, \sigma} \Psi_k^{\sigma, pd}, \quad (7)$$

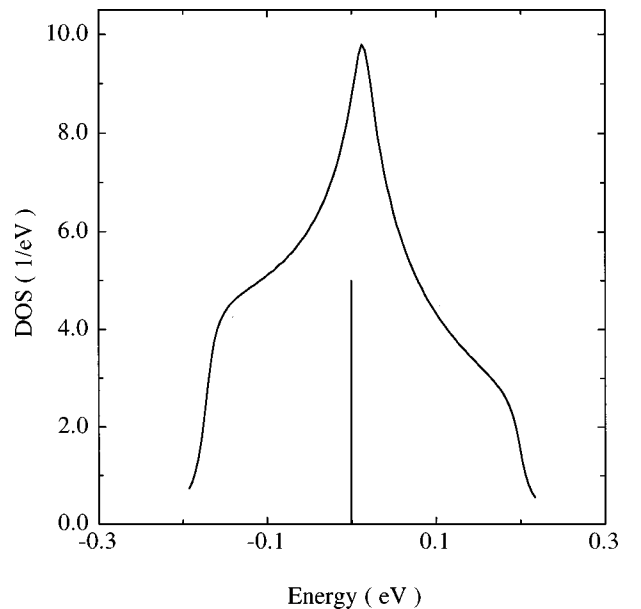


FIG. 1. Density of states of the singlet bonding band for $T^* = 180$ K. The vertical line marks the position of the chemical potential for the hole concentration of $\delta = 0.33$.

where

$$G_0(Q) = \sum' \frac{2|V(Q)|^2 \hbar \omega_Q}{(\varepsilon_k - \varepsilon_{k+Q})^2 - (\hbar \omega_Q)^2} \langle \Psi_{k+Q}^{pd,\uparrow} \Psi_k^{\uparrow,pd} \rangle \quad (8)$$

and

$$G_1(k, Q) = \frac{2|V(Q)|^2 \hbar \omega_Q}{(\varepsilon_k - \varepsilon_{k+Q})^2 - (\hbar \omega_Q)^2} \sum \langle \Psi_{k'+Q}^{pd,\uparrow} \Psi_{k'}^{\uparrow,pd} \rangle. \quad (9)$$

The primed sum in $G_0(Q)$ runs over states which satisfy the conditions²⁸ $|\varepsilon_k|$, $|\varepsilon_{k+Q} - \varepsilon_k| < \hbar \omega_D$, where ω_D is the Debye frequency, and $V(Q)$ is the parameter of the hole-phonon interaction.

As can be seen from Eqs. (8) and (9), the momentum dependence of the parameter $G_k = G_0(Q) + G_1(k, Q)$ can be written as follows:

$$G_k = \sum \left[A(\omega_Q) - B(\omega_Q) \times \frac{(\hbar \omega_Q)^2 \Theta(\hbar \omega_D - |\varepsilon_k|) \Theta(\hbar \omega_D - |\varepsilon_k - \varepsilon_{k+Q}|)}{(\varepsilon_k - \varepsilon_{k+Q})^2 - (\hbar \omega_Q)^2} \right], \quad (10)$$

where ω_Q are the frequencies of the phonon modes being active in the CDW transition. For simplicity, we restricted ourselves to the so-called breathing phonon mode only, $\hbar \omega_Q = 42$ meV. Θ denote the ordinary Θ functions which equal 1 in the case of $|\varepsilon_k|$, $|\varepsilon_{k+Q} - \varepsilon_k| < \hbar \omega_D$ and which are 0 elsewhere. The parameters $A(\omega_Q)$ and $B(\omega_Q)$ are determined by

$$A(\omega_Q) = C \sum \frac{f(E_{1k}) - f(E_{2k})}{E_{1k} - E_{2k}} \times \frac{G_k \Theta(\hbar \omega_D - |\varepsilon_k|) \Theta(\hbar \omega_D - |\varepsilon_k - \varepsilon_{k+Q}|)}{(\varepsilon_k - \varepsilon_{k+Q})^2 - (\hbar \omega_Q)^2}, \quad (11)$$

$$B(\omega_Q) = -\frac{C}{(\hbar \omega_Q)^2} \sum \frac{f(E_{1k}) - f(E_{2k})}{E_{1k} - E_{2k}} G_k, \quad (12)$$

where

$$E_{1k,2k} = \frac{\varepsilon_k + \varepsilon_{k+Q}}{2} \pm \frac{1}{2} [(\varepsilon_k - \varepsilon_{k+Q})^2 + 4(PG_k)^2]^{1/2} \quad (13)$$

denote the energy dispersion branches and $C = 2|V(Q)|^2 \hbar \omega_Q P^2$. Using our recent NMR data,⁹ we suggest that the CDW transition temperature, T^* , is 180 K. Equations (11) and (12) were solved numerically by the iteration procedure in the temperature region $T_c < T < T^*$ for the half-filled band. The temperature dependence of both $A(\omega_Q)$ and $B(\omega_Q)$ can be described by the function $\sqrt{1 - (T/T^*)^2}$ with the following numerical values: $B(\omega_Q)/A(\omega_Q) = 0.88$, $A(\omega_Q) = 17$ meV, and $V(Q) = 109$ meV.

It is easy to show²⁹ that the breathing oxygen mode coupling constant, $V(Q)$, at $Q = \pi$ is given by

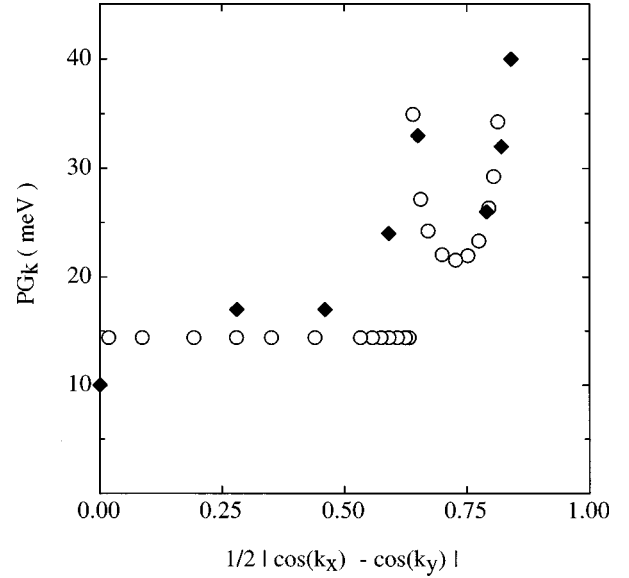


FIG. 2. Open circles: Calculated momentum dependence of the pseudogap PG_k at $T = 170$ K. Rhombus: Experimental points for $\text{Bi}_2\text{Sr}_2\text{CaCu}_2\text{O}_{8+y}$ (taken from Ref. 2). All experimental points were shifted up by 14 meV.

$$V(Q) = 2V' \sqrt{\frac{\hbar}{2M\omega_Q}}, \quad (14)$$

where V' is the derivative, with respect to the copper position, of the Zhang-Rice singlet energy taken over the normal coordinate of the breathing vibration of the oxygen plaquette. M is the mass of the unit cell, i.e., two oxygen masses in our case. According to our earlier estimates,^{30,31} $V' = 1.5$ eV/Å and consequently Eq. (14) yields $V(Q) = 117$ meV which agrees quite well with the value we had obtained above via Eqs. (11) and (12). This agreement supports the idea that the CDW transition is caused by the breathing oxygen mode in the Cu-O₂ plane. That the breathing mode can lead to a CDW transition in the Cu-O chain, has been shown recently.³²

Of course, other microscopic mechanisms are feasible that lead to the transition. For example, in the original paper,¹⁰ where the spin gap phenomenon was proposed to be caused by a transition due to CDW, the *tilting* mode motion was suggested. Simanovskiy and Klein³³ proposed the scattering of the carriers by the tunneling zig-zag motion on copper-oxygen chains as a mechanism for the superconductivity transition. However, in both cases, it is not clear yet how to get such a large value of $V(Q)$.

The momentum dependence of the calculated gap function, PG_k , is shown in Fig. 2 together with photoemission data.² Although we have considered only one phonon mode, the calculated gap exhibits the main features of the experimental data. For $0.5(\cos k_x - \cos k_y)$ values from 0 to 0.6, the gap has a constant value, PG_0 , in agreement with experiment. Above 0.6, where $G_1(k, Q)$ is different from 0, the gap increases in accordance with the experimental data. The appearance of the peak near 0.6 is due to selecting one phonon mode only; inclusion of several modes would smear out the peak.

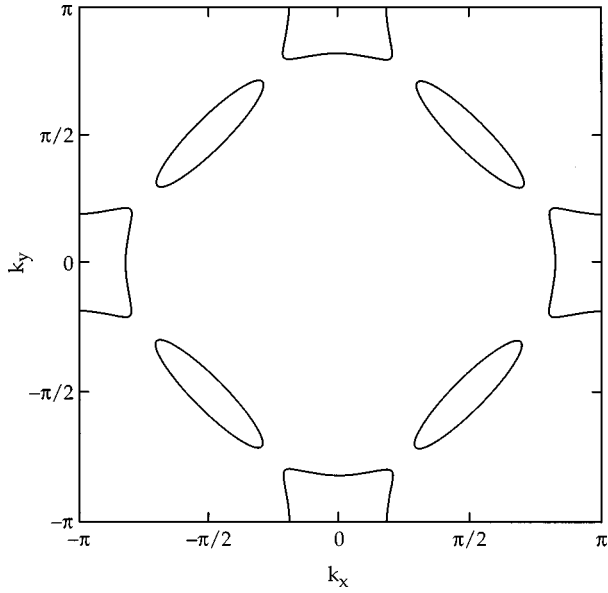


FIG. 3. Calculated Fermi surface at $T=170$ K.

The evolution of the Fermi surface (FS) is illustrated in Fig. 3. When the CDW gap opens the corresponding part of the FS disappears, it shrinks to the so-called pockets centered at $(\pm \pi/2, \pm \pi/2)$. This result was observed in a photoemission experiment³⁴ in $\text{Bi}_2\text{Sr}_2\text{CaCu}_2\text{O}_{8+y}$. However, we found a pattern around the points $(\pm \pi, 0)$, $(0, \pm \pi)$ which had not been mentioned in Ref. 34. Thus, this prediction of our calculation should be examined in future experiments.

We now discuss the role played by the order parameter fluctuations $|G_k|$. Following Chap. 7 of Gruner's book,¹² it is useful to rewrite $|G_k|$ in the form

$$G_k(Q) = G_k^{(0)}(1 + \cos 2\Phi), \quad (15)$$

where $G_k^{(0)}$ and Φ are the modul and phase of the order parameter, respectively. In a CDW instability, the phase rather than the modul fluctuations are dominant.¹² As one can see from Eq. (13), the fluctuation Φ yields, to the pseudogap in the normal state, an additional contribution which is dominating in the 1D case.²⁵ The correlation length of the fluctuation radius²⁹ is given by

$$\xi = \xi_0 \sqrt{\frac{T^*}{T - T^*}} \quad (16)$$

and it goes up near T^* . Thus, the Fermi surface pattern can be washed out slightly around T^* and T^* itself can be "smeared" out.

IV. SPIN SUSCEPTIBILITY

Starting from Eq. (13) and in analogy to the case $T > T^*$ (Ref. 35), we obtained the following expression for the spin susceptibility in the fast fluctuating regime:

$$\chi(\delta, \theta) = \frac{(1 + \delta)^2 \chi_{\text{Pauli}}(\delta, \theta)}{4\delta - Z(\delta, \theta)}, \quad (17)$$

where $\chi_{\text{Pauli}}(\delta, \theta)$ is the typical Pauli-Lindhard susceptibility for the usual Fermi liquid:

$$\chi_{\text{Pauli}}(\delta, \theta) = -\frac{1}{2N} (g\beta)^2 \sum \left[C_{1k} \frac{\partial f(E_{1k})}{\partial E_{1k}} + C_{2k} \frac{\partial f(E_{2k})}{\partial E_{2k}} \right]. \quad (18)$$

The doping dependent prefactor $(1 + \delta)^2$ and the denominator in Eq. (17) reflect the non-Fermi liquid behavior of the singlet band. The coefficients C_{1k} and C_{2k} in Eq. (18) are

$$C_{1k} = \frac{E_{1k} - \varepsilon_{k+Q}}{E_{1k} - E_{2k}}, \quad C_{2k} = \frac{-E_{2k} + \varepsilon_{k+Q}}{E_{1k} - E_{2k}}. \quad (19)$$

The function $Z(\delta, \theta)$ is determined by

$$Z(\delta, \theta) = -\frac{(1 + \delta)^2}{2N} \sum \left[C_{1k} Y_{1k} \frac{\partial f(E_{1k})}{\partial E_{1k}} + C_{2k} Y_{2k} \frac{\partial f(E_{2k})}{\partial E_{2k}} \right], \quad (20)$$

where

$$Y_{1k,2k} = \frac{4(E_{1k,2k} + \mu)}{(1 + \delta)} - \frac{4J}{(1 + \delta)^2} [1 - 4\langle S_i S_j \rangle_1 + 2\delta] + 32F\delta. \quad (21)$$

Here, J is the parameter of the spin-spin coupling between Cu(2) spins in the plane and $\langle S_i S_j \rangle_1$ is the spin correlation function for the first copper neighbors. It is widely believed that the antiferromagnetic correlations are very strong in HTSC cuprates.¹ Following Ref. 36, we put $\langle S_i S_j \rangle_1 = -0.08$ and we take $F = 4$ meV from our earlier estimates.²⁰

The choice of the numerical value for J is based on the following observations. Recent neutron scattering experiments³⁷ in undoped $\text{YBa}_2\text{Cu}_3\text{O}_{6.15}$ determined $J = 125$ meV. With doping, J decreases due to the ferromagnetic RKKY coupling via carriers. For instance, the inelastic neutron scattering experiments for $\text{YBa}_2\text{Cu}_3\text{O}_{6+x}$, where $0.65 < x < 0.92$, have been successfully explained³⁸ with $J = 25$ meV. Out of this broad range of J values, we have chosen $J = 70$ meV in order to get the best fit to the experimental curve. The results of our calculations are shown in Fig. 4 together with experimental points deduced from the planar Cu Knight shift.¹⁷ Obviously, the agreement is remarkably good.

V. EFFECT OF DOPING AND ISOTOPE MASSES ON T^*

We will now discuss two important consequences of our model, namely the dependence of the CDW transition temperature, T^* , on doping and isotope masses.

A. Doping dependence

It is known³⁹ that the superconductivity transition temperature, T_c , is highest when the chemical potential is situated at the peak of the DOS (so-called Van Hove scenario). On the other hand, the best condition for the CDW transition, i.e., the highest T^* , is a half-filled band.^{28,10} In underdoped samples, T^* is larger than T_c because the position of the chemical potential is close to the half-filling regime, but it is still far from the saddle singularity peak. If we increase the

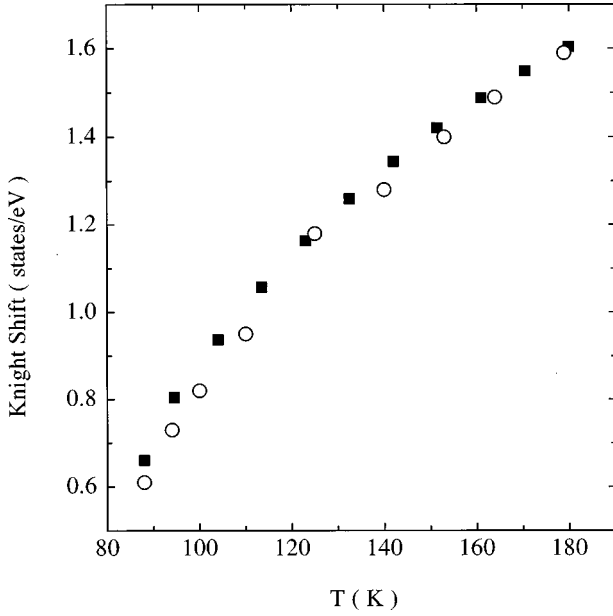


FIG. 4. Temperature dependence of the spin susceptibility for Cu(2) in the plane (magnetic field $\perp c$ axis) in $\text{YBa}_2\text{Cu}_4\text{O}_8$. Squares: calculated values; circles: experimental data (taken from Ref. 17).

doping level towards a value which is optimal for T_c and T^* , then both quantities are interchanged, that means T^* becomes smaller than T_c .

In order to calculate the doping dependence of T^* , we must take into account that the width of the singlet correlated band depends on the doping level, δ , in two respects: first, because of the factor $P=(1+\delta)/2$ in Eq. (2) and, second, because the hopping integral, t_1 , depends on δ via the spin-spin correlation function, $\langle S_i S_j \rangle_1$. If only first neighbors are considered, t_1 can be written as³⁶

$$t_1 = t_1^0 \left(1 + \frac{\langle S_i S_j \rangle_1}{P^2} \right), \quad (22)$$

where t_1^0 is independent of δ . Obviously, the antiferromagnetic fluctuations reduce the effective value of the nearest copper spins hopping integral. Recently, this effect has been discussed in Refs. 40 and 41, and references therein.

Using results of Ref. 36 and the experimentally determined doping dependence of the magnetic correlation length in $\text{La}_{2-x}\text{Sr}_x\text{CuO}_4$ (Ref. 42, see also Ref. 43 as a review), we found the doping dependence of $\langle S_i S_j \rangle_1$ which is listed in Table II. Using our values for $B(\omega_Q)/A(\omega_Q)$, $V(Q)$, and ω_Q (see Sec. III), which were calculated for the half-filled band, we solve Eqs. (11) and (12) self-consistently for different doping levels, thus obtaining the doping dependence of T^* .

Figure 5 presents the calculated transition temperatures, T^* , as a function of the doping level. With increasing doping $\delta/2$ (hole concentration per *one* copper site), T^* lowers from

TABLE II. Values of the spin-spin correlation function (first neighbors) for different doping.

$\langle S_i S_j \rangle_1$	0.00	-0.08	-0.10
δ	0.40	0.33	0.20

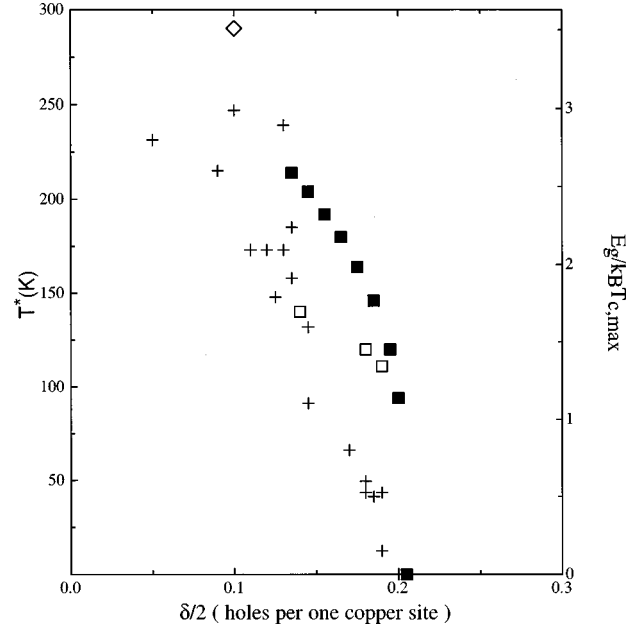


FIG. 5. Doping dependence of T^* and E_g . Black squares: Calculated T^* values. The other symbols denote experimental $E_g/k_B T_{c,\max}$ values (where $T_{c,\max}=82.6$ K) deduced from Cu NMR (Ref. 45) (open squares), Y NMR (Ref. 44) (crosses), and photoemission spectroscopy (Ref. 2) (rhombus).

a maximum value at 0.13 almost linearly until the chemical potential corresponds to the singularity peak in the DOS ($\delta/2=0.2$). At this doping level, the CDW transition temperature coincides with T_c . If the doping is increased further, T^* decreases enormously and becomes zero at already $\delta/2=0.205$.

In Fig. 5, we have also included the doping dependence of the normalized pseudogap, $E_g/k_B T_{c,\max}$, where $T_{c,\max}=82.6$ K. Because of the large scatter of experimental data, we only considered values which were deduced from Y NMR shifts,⁴⁴ Cu NMR shifts,⁴⁵ and photoemission.² T^* and E_g increase almost linearly with decreasing doping. At $\delta/2=0.2$, $T^*=86$ K which is close to $T_{c,\max}$. This implies $E_g=0$ as observed experimentally. The overall agreement between theoretical and experimental data demonstrates that the CDW scenario is able to explain qualitatively the doping dependence of E_g , at least near the optimal doping level.

Since our model is based on the condition $4t_1 > J$, it cannot be applied at low doping levels where $J > 4t_1$. In this region, the CDW instability scenario probably crosses over into a SDW one and the calculation requires to take into account the so-called precursors of the valence and conduction band pseudosplitting of the magnetically ordered state.⁴⁶ This topic is beyond the scope of the present paper.

B. Isotope dependence

The most crucial experimental verification whether the pseudogap is due to a CDW or SDW instability, is probably the measurement of the isotope effect, i.e., the change, ΔT^* , of the critical temperature resulting from a change, Δm , of the isotope composition and its dependence on doping level. We have calculated ΔT^* with the help of Eqs. (11) and (12) for the case that ^{16}O is replaced by ^{18}O . The result, in the

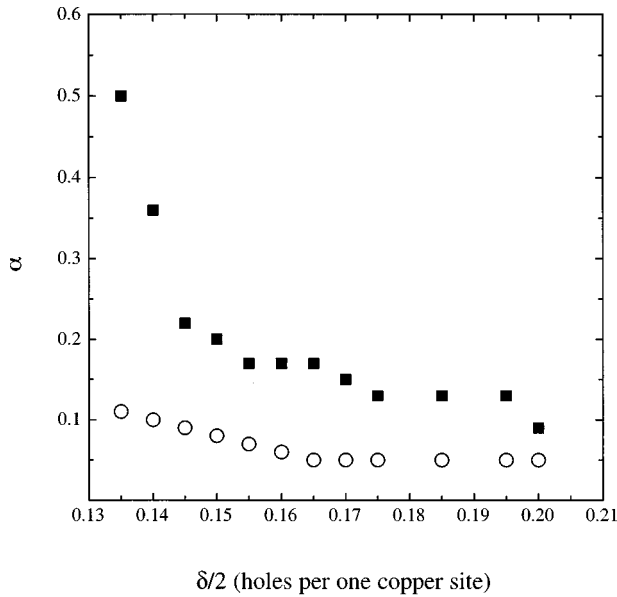


FIG. 6. Calculated α values (squares) and α_0 values (circles, taken from Ref. 39).

form of the isotope coefficient $\alpha = (-\Delta T^*/T^*)(m/\Delta m)$, is plotted in Fig. 6. For comparison, we have also included the coefficient $\alpha_0 = -(\Delta T_c/T_c)(m/\Delta m)$ calculated by Nazarenko and Dagotto³⁹ in the so-called Van Hove scenario.

Since our Eqs. (8) and (9), on which the calculation of the critical temperature of the CDW gap is based, have the same features as the respective analytical formulas deduced by Balsiero and Falicov,²⁸ one expects a similar behavior of α_0 and α with respect to the suppression by the Van Hove singularity. In the case of T_c , the suppression is a factor of 10

compared to the ordinary BCS value.²⁸ Our calculations show that α is strongly suppressed too if the chemical potential coincides with the saddle singularity peak. However, when the chemical potential moves away from the peak, α increases and reaches already a value of 0.5 for a doping level of $\delta/2=0.13$.

VI. CONCLUSION

We have examined, for the normal state of layered cuprates, the CDW scenario for the pseudogap which opens at a temperature T^* . Using the singlet band model for the normal state we explain the important features of the momentum and temperature dependences of the pseudogap. We have shown that the CDW instability explains the strong temperature dependence of the spin susceptibility in $\text{YBa}_2\text{Cu}_4\text{O}_8$ in the temperature range $T_c < T < T^*$. The doping dependence of the CDW transition temperature and of the pseudogap formation temperature qualitatively agree. Two important predictions of our calculation are the following: (1) Below T^* , the Fermi surface shrinks into pockets at $(\pm \pi/2, \pm \pi/2)$, and remnant squarelike patterns near the point $(0, \pm \pi)$, $(\pm \pi, 0)$ of the Brillouin zone. (2) T^* exhibits an isotope effect. An experimental verification of this prediction is in progress.

ACKNOWLEDGMENTS

I. Eremin and M. Eremin are grateful to Professor V. Meyer and E. Staub for hospitality during our stay at Zurich University where this work was performed. Our work was supported by the Swiss National Science Foundation and the Russian Scientific Council on HTSC (No. 94029).

- ¹D. Pines and P. Monthoux, *J. Phys. Chem. Solids* **56**, 1651 (1995).
- ²A. G. Loeser, Z.-X. Shen, D. S. Dessau, D. S. Marshall, C. H. Park, P. Fournier, and A. Kapitulnik, *Science* **273**, 325 (1996).
- ³H. Ding, T. Yokoya, J. C. Campuzano, T. Takahashi, M. Randeria, M. R. Norman, T. Mochiku, K. Kadowaki, and J. Giapintzakis, *Nature (London)* **382**, 51 (1996).
- ⁴W. Y. Liang, J. W. Loram, K. A. Mirza, N. Athanassopoulou, and J. R. Cooper, *Physica C* **263**, 277 (1996).
- ⁵A. P. Litvinchuk, C. Thomsen, and M. Cardona, *Solid State Commun.* **83**, 343 (1992).
- ⁶E. Kaldis, H. Schwer, and J. Karpinski, in *Anharmonic Properties of High- T_c Cuprates*, edited by D. Mihailovic, G. Ruani, E. Kaldis, and K. A. Muller (World Scientific, Singapore, 1995), p. 105.
- ⁷M. Mali, J. Roos, and D. Brinkmann, *Phys. Rev. B* **53**, 3550 (1996).
- ⁸O. N. Bakharev, A. V. Dooglav, A. V. Egorov, E. V. Krjukov, Yu. A. Sakhratov, and M. A. Teplov, *Pis'ma Zh. Eksp. Teor. Fiz.* **64**, 365 (1996) [*JETP Lett.* **64**, 399 (1996)].
- ⁹A. Suter, M. Mali, J. Roos, D. Brinkmann, J. Karpinski, and E. Kaldis, *Phys. Rev. B* **56**, 5542 (1997).
- ¹⁰R. S. Markiewicz, *Physica C* **193**, 323 (1992).
- ¹¹Claire Schlenker, in *Physics and Chemistry of Low-Dimensional*

Inorganic Conductors, edited by Claire Schlenker *et al.* (Plenum Press, New York, 1996).

- ¹²G. Gruner, *Density Waves in Solids* (Addison-Wesley, Reading, MA, 1994).
- ¹³Z.-X. Shen and D. S. Dessau, *Phys. Rep.* **253**, 1 (1995).
- ¹⁴H. L. Edwards, A. L. Barr, J. T. Markert, and A. L. de Lozanne, *Phys. Rev. Lett.* **73**, 1154 (1994).
- ¹⁵R. A. Klemm, *Layered Superconductors* (Oxford University Press, New York, 1997).
- ¹⁶R. S. Markiewicz, *Phys. Chem. Solids* **58**, 1179 (1997).
- ¹⁷M. Bankay, M. Mali, J. Roos, and D. Brinkmann, *Phys. Rev. B* **50**, 6416 (1994).
- ¹⁸F. C. Zhang and T. M. Rice, *Phys. Rev. B* **37**, 3759 (1988).
- ¹⁹M. V. Eremin, R. Markendorf, and S. V. Varlamov, *Solid State Commun.* **88**, 15 (1993); M. V. Eremin, S. G. Solovjanov, S. V. Varlamov, D. Brinkmann, M. Mali, R. Markendorf, and J. Roos, *JETP Lett.* **60**, 125 (1994).
- ²⁰M. V. Eremin and E. Sigmund, *Solid State Commun.* **90**, 795 (1994).
- ²¹M. V. Eremin, S. G. Solovjanov, and S. V. Varlamov, *J. Phys. Chem. Solids* **56**, 1713 (1995).
- ²²K. Gofron, J. C. Campuzano, H. Ding, C. Gu, R. Liu, B. Dabrowski, B. W. Veal, W. Cramer, and G. Jennings, *J. Phys. Chem. Solids* **54**, 1193 (1993).

- ²³M. G. Stachiotti, C. R. A. Catlow, C. O. Rodriguez, and N. E. Christensen, *Physica C* **269**, 273 (1996).
- ²⁴Matthias C. Schabel, C.-H. Park, A. Matsuura, Z. X. Shen, D. A. Bonn, Ruixing Liang, and W. N. Hardy, *Phys. Rev. B* **55**, 2796 (1997).
- ²⁵P. A. Lee, T. M. Rice, and P. W. Anderson, *Phys. Rev. Lett.* **31**, 462 (1973).
- ²⁶Y. Hasegawa and H. Fukuyama, *J. Phys. Soc. Jpn.* **55**, 3978 (1986).
- ²⁷K. Maki, *Phys. Rev. B* **41**, 9308 (1990).
- ²⁸C. A. Balseiro and L. M. Falicov, *Phys. Rev. B* **20**, 4457 (1979).
- ²⁹L. D. Landau and E. M. Lifshitz, *Statistical Physics* (Pergamon Press, London, 1958).
- ³⁰M. V. Eremin, *Z. Naturforsch. Teil A* **49**, 385 (1994).
- ³¹I. Eremin and A. Larionov, *Fiz. Tverd. Tela (Leningrad)*, **38**, 930 (1996) [*Phys. Solid State* **38**, 513 (1996)].
- ³²R. Fehrenbacher, *Phys. Rev. Lett.* **77**, 2288 (1996).
- ³³S. Simanovsky and M. W. Klein, *Phys. Rev. B* **54**, 7430 (1996).
- ³⁴D. S. Marshall, D. S. Dessau, A. G. Loeser, C.-H. Park, A. Y. Matsuura, J. N. Eckstein, I. Bozovic, P. Fournier, A. Kapitulnik, W. E. Spicer, and Z.-X. Shen, *Phys. Rev. Lett.* **76**, 4841 (1996).
- ³⁵M. V. Eremin, S. G. Solovjanov, S. V. Varlamov, and I. M. Eremin, *Proceedings of the 10th Anniversary of the Workshop on Physics, Materials and Application HTSC*, Houston, Texas, 1996 (World Scientific, Rivers Edge, NY, 1996) p. 517; M. V. Eremin, S. V. Varlamov, I. Eremin, D. Brinkmann, M. Mali, R. Markendorf, and J. Roos, *Physica B* **230-232**, 952 (1997); I. Eremin, *ibid.* **234-236**, 792 (1997).
- ³⁶N. M. Plakida, R. Hayn, and J. L. Richard, *Phys. Rev. B* **51**, 16 599 (1995).
- ³⁷S. M. Hayden, G. Aeppli, T. G. Perring, H. A. Mook, and F. Dogan, *Phys. Rev. B* **54**, R6905 (1996).
- ³⁸G. Blumberg, B. P. Stojkovic, and M. V. Klein, *Phys. Rev. B* **52**, R15 741 (1995).
- ³⁹A. Nazarenko and E. Dagotto, *Phys. Rev. B* **53**, R2987 (1996).
- ⁴⁰R. Hayn, A. F. Barabanov, J. Schulenburg, and J. Richter, *Phys. Rev. B* **53**, 11 714 (1996).
- ⁴¹V. I. Belinicher, A. L. Chernyshev, and V. A. Shubin, *Phys. Rev. B* **53**, 335 (1996).
- ⁴²T. R. Thurston, R. J. Birgeneau, M. A. Kastner, N. W. Preyer, G. Shirane, Y. Fujii, K. Yamada, Y. Endoh, K. Kakurai, M. Matsuda, Y. Hidaka, and T. Murakami, *Phys. Rev. B* **40**, 4585 (1989).
- ⁴³V. Barzykin and D. Pines, *Phys. Rev. B* **52**, 13 585 (1995).
- ⁴⁴G. W. M. Williams, J. L. Tallon, R. Michalak, and R. Dupree, *Phys. Rev. B* **54**, R6909 (1996).
- ⁴⁵M. Matsumura, Y. Sakamoto, T. Fushihara, Y. Itoh, and H. Yamagata, *J. Phys. Soc. Jpn.* **64**, 721 (1995).
- ⁴⁶A. V. Chubukov, D. Pines, and B. P. Stojkovic, *J. Phys. Condens. Matter* **8**, 1 (1996).